Magnetization reversal and dynamics in non-interacting NiFe mesoscopic ring arrays

M. Kaur, S. Husale, D. Varandani, A. Gupta, T. D. Senguttuvan, B. R. Mehta, and R. C. Budhani

Citation: Journal of Applied Physics **115**, 163905 (2014); doi: 10.1063/1.4872139
View online: http://dx.doi.org/10.1063/1.4872139
View Table of Contents: http://scitation.aip.org/content/aip/journal/jap/115/16?ver=pdfcov
Published by the AIP Publishing

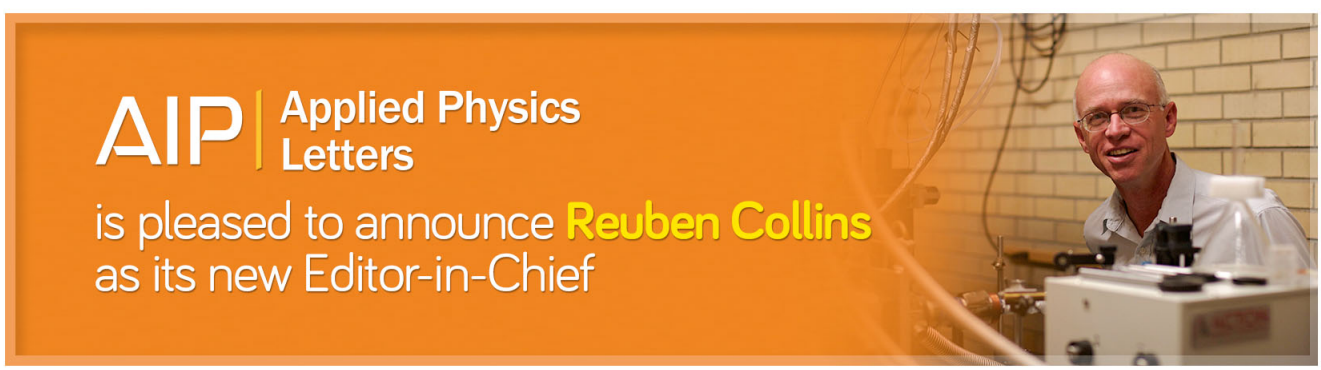

Magnetization reversal and dynamics in non-interacting NiFe mesoscopic ring arrays

M. Kaur,[1] S. Husale,[1] D. Varandani,[2] A. Gupta,[1] T. D. Senguttuvan,[1] B. R. Mehta,[2] and R. C. Budhani[1,a)]
[1]*Quantum Phenomena and Applications Division, National Physical Laboratory, Council of Scientific and Industrial Research, New Delhi 110012, India*
[2]*Indian Institute of Technology Delhi, New Delhi 110016, India*

(Received 28 March 2014; accepted 9 April 2014; published online 24 April 2014)

The dynamics of magnetization (M) reversal and relaxation as a function of temperature (T) are reported in three non-interacting NiFe ring arrays having fixed ring outer diameter and varying widths. Additionally, the dependence of M(H) loop on the angle (θ) between magnetic field (H) and the plane of the rings is addressed. The M(H) loops show a double step transition from onion state (OS) to vortex state (VS) at all temperatures (T = 3 to 300 K) and angles ($\theta = 0$ to 90°). The critical reversal fields H_{C1} (OS to VS) and H_{C2} (VS to OS) show a pronounced dependence on T, ring width, and θ. Estimation of the transverse and vortex domain wall energies reveals that the latter is favored in the OS. The OS is also the remanent state in the smallest rings and decays with the effective energy scale (U_0/T) of 50 and 32 meV/K at 10 and 300 K, respectively. The robust in-plane anisotropy of magnetization of ring assemblies is established by scaling the M(H) with θ.
 [http://dx.doi.org/10.1063/1.4872139]

I. INTRODUCTION

Magnetic films patterned into mesoscopic elements opened a new research area to understand the physics of magnetic dynamics in them, besides the potential in the applied area of magnetic storage devices.[1,2] Past several years have witnessed a keen theoretical and experimental interest in magnetic patterns of various shapes and dimensions constituted of discs,[2,3] dots,[4] rings,[5–7] squares,[8,9] and rectangles[9] as base units. The magnetostatic interactions in the neighbouring magnetic elements and their dependence on the specific geometry of the patterns and magnetic states in them have been some of the key issues.[10] The technological importance of magnetic vortex state (VS) having zero stray field in disc geometry was realized, only to be limited by its highly energetic core raising the problem of the VS stability. Subsequently, the removal of the core in ring geometries looked promising to produce stable VS with enhanced switching behavior and high packing density.[11]

In patterned magnetic rings, besides a VS, an additional "onion state" (OS) characterized by two diametrically opposite domain walls (DW) was discovered.[5] The OS to VS transition was found to be highly dependent on the edge to edge distance of the rings.[12–14] It was shown that beyond a critical distance the magnetostatic interactions between adjacent elements become insignificant, leading to a radical change in the DW dynamics. In case of NiFe ring arrays, the observed critical distance was >100 nm.[13] We report detailed magnetization measurements as a function of ring width (W), temperature (T), angle (θ), and time (t) in arrays of non-interacting permalloy rings (edge to edge distance ~ 1.2 μm) that have been lacking till now. The present work reveals double stepped OS to VS transition in such lattices with switching dynamics determined mainly by diagonally opposite vortex type domain walls characterizing the OS.

II. EXPERIMENTAL

Permalloy ($Ni_{80}Fe_{20}$) rings were fabricated on silicon wafers using electron beam lithography and lift-off. We have used bilayer resist consisting of polymethyl methacrylate (PMMA) and methyl methacrylate (MMA). Electron beam lithography was done using Zeiss Auriga driven by the digital pattern generator of Raith Elphy multi-beam system. Ring assemblies having ring widths of 340, 500, and 660 nm with fixed center to center distance of 2.8 μm and outer diameter (OD) of 1.6 μm spread over an area of 9 mm^2 were created on the photoresist. Permalloy films of thickness (t) ~ 45 nm were deposited on the patterned SiO_2/Si substrate by DC magnetron sputtering at 2×10^{-3} millbars of Argon and 28 W power. A thin layer (3–5 nm) of titanium was deposited first by sputtering as an adhesive layer. These films were then kept overnight in acetone for complete lift off. The samples having ring width 660, 500, and 340 nm are referred to as S660, S500, and S340, respectively, in the following discussion. For comparison, a plain film of permalloy having same thickness was also deposited on bare SiO_2/Si substrate in the same deposition run.

The surface morphology and ring dimension measurements were carried out by imaging all the samples in a scanning electron microscope (SEM). The magnetization M(H, T, θ, t) was measured using a superconducting quantum interference device (SQUID) based magnetometer (Quantum Design MPMS-7) in field range H ~ 0 to ±0.1 T, temperature range T ~ 3 to 300 K, window of time t ~ 3 h, and angle ~ 0 to 90° (where $\theta = 0°$ corresponds to H//ring-plane). The magnetic force microscopy (MFM) of the S340 sample was carried out with MFM tip to sample distance ~45 nm.

a)Author to whom correspondence should be addressed. Electronic mail: rcb@nplindia.org. Tel. +91-11-45609201. FAX: +91-11-4560310.

III. RESULTS AND DISCUSSION

Figs. 1(a), 1(c), and 1(e) show the SEM micrograph depicting array of rings with desired dimension for S660, S500, and S340 samples, respectively. The corresponding M(H) loops measured at T = 3 and 300 K with in-plane field are shown in Figs. 1(b), 1(d), and 1(f). The saturation magnetization (M_s) of the plain film is 3.84×10^{-4} emu (see the inset of Fig. 1(b)), which is close to the expected value of 3.24×10^{-4} emu and confirms the quality of the film.[13] The M_s of the ring samples is found to scale with the effective volume of the respective ring arrays. The critical features of the M(H) loop, marked by noticeable change in the slope at points A, B, C, D, and E, can be related to OS, VS and reverse OS formation in the rings. Well above point A, the rings are in single domain (SD) saturated state (inset of Fig. 1(d)). Decreasing the field leads to a reversible OS (inset of Fig. 1(d)). The point A marks the onset of hysteretic two step OS to VS transition characterized by regions A to B and B to C. Experimental hint of a similar OS to VS transition has been reported earlier.[15] The plateau between C and D indicates the existence of VS (see the inset of Fig. 1(f)) and the region D to E depicts the VS to reverse OS transition.

For the S660 sample, as seen along the + H to − H trajectory of the M(H) in Fig. 1(b), the OS to VS transition occurs above the zero field at both T = 3 and 300 K. For the smaller ring width (S500 sample), the same transition shifts from above zero field at 300 K to negative fields at 3 K (see Fig. 1(d)). On decreasing the ring width further (S340 sample), the transition occurs in the negative field region at both T = 3 and 300 K (see Fig. 1(f)). These results clearly show that only sample S340 exhibits OS as the remanent state at 300 K. This is confirmed by the room temperature MFM studies. The MFM image of the S340 in the demagnetized (remanent-magnetized) state as established by cycling the sample between +0.1 and −0.1 T (+0.1 to 0 T) is shown in Fig. 2(a) (Fig. 2(b)). The inset of Fig. 2(b) clearly reveals the presence of diagonally opposite bright and dark regions in the ring demonstrating the formation of OS.

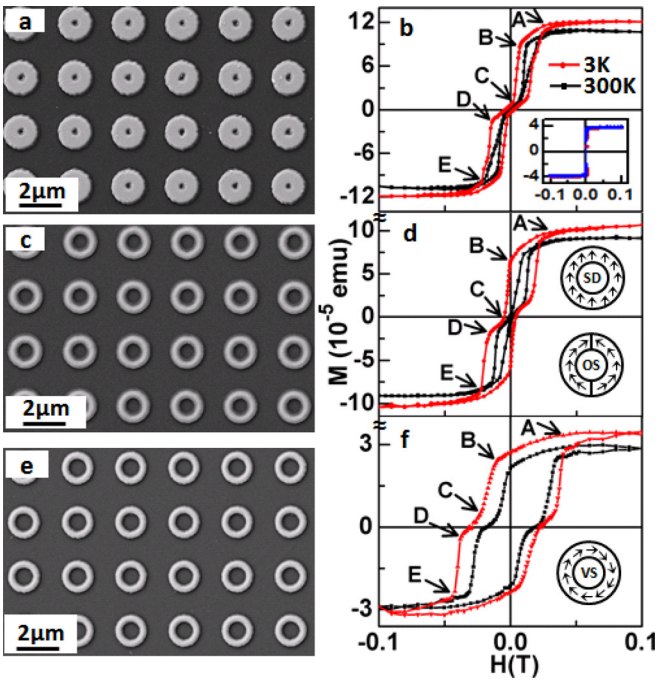

FIG. 1. SEM images and M(H) loops for the ring samples: (a) and (b) S660; (c) and (d) S500; (e) and (f) S340. The points A to E mark pronounced change of slope in the M(H) curves. The inset (b) shows M(H) loop of a plain film. Schematics of SD and OS are shown as inset (d) and VS as inset (f).

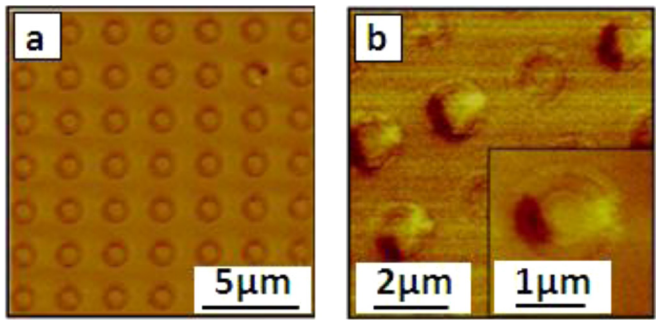

FIG. 2. MFM images of S340 ring sample in: (a) demagnetized state and (b) remanent magnetized state. Inset (b) shows a magnified MFM image of single ring in remanent OS.

The critical reversal fields H_{C1} and H_{C2} that mark the beginning and the end of the VS are defined by points C and D (see Figs. 1(b), 1(d), and 1(f)), respectively. For all the ring samples, the variation of H_{C1} and H_{C2} as a function temperature are plotted in Figs. 3(a) and 3(b), respectively. For all the ring widths, both H_{C1} and H_{C2} increase with decrease in temperature, which becomes pronounced below ~25 K. For all temperatures, both the critical reversal fields increase with decrease in ring width, (compare the data along the vertical lines in Figs. 3(a) and 3(b)). The latter observation has been also been reported in Co-based rings at room temperature.[16,17] To understand these results, we need to look at the dynamics of the double stepped OS to VS transition in our ring samples (Figs. 1(b), 1(d), and 1(f)). Just above point A, there exists a reversible OS with two diagonally opposite transverse domain walls (TDWs). Reducing the field below point A results in a change of slope of M(H) indicating either the growth of TDW or nucleation of a Vortex Domain Wall (VDW), see the inset of Fig. 3(d).[13,18] In head to head TDW, the spins rotate 180° within the ring plane itself from one head to the other over the

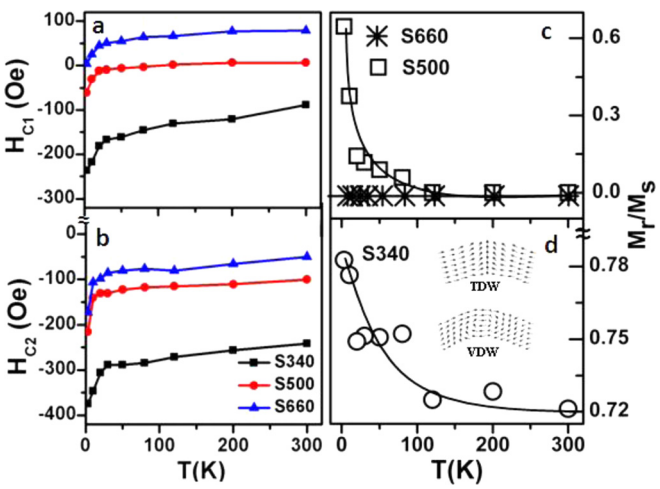

FIG. 3. (a) H_{C1} and (b) H_{C2} as a function of temperature for the three ring samples. (c) and (d) show the ratio of M_r/M_s as a function of temperature for the same samples. Schematics of TDW and VDW are shown as inset (d).

DW. In head-to-head VDW the spins rotate clockwise from one head and anticlockwise from the other head around a core. Considering the fact that edge to edge ring distance in all the three samples is 1.2 μm, the suppressed inter-ring magnetostatic interactions are expected to favor the formation of VDW instead of TDW.[13] As per the micromagnetic simulations, the multiple stepped nature of OS to VS transition also points out formation and dynamics of VDW.[15,19] The favorable configuration can be quantitatively understood by the DW energetic. In the present case of polycrystalline permalloy rings, we can neglect the contribution of anisotropy energy, thus leaving only the exchange (E_{ex}) and magnetostatic (E_{ms}) energy contributions to the free energy. The respective energy difference between VDW (E_{vortex}) and TDW (E_{trans}) are given by following equations:[13,18]

$$(E_{vortex} - E_{trans})_{ex} \approx 2\pi t A \ln\left(\frac{r_{max}}{r_{min}}\right), \quad (1)$$

$$(E_{vortex} - E_{trans})_{ms} \approx -\frac{1}{8}\mu_0 M_s^2 t^2 W, \quad (2)$$

where t and W are the ring thickness and width, respectively; A is the exchange constant ($\sim 1.3 \times 10^{-11}$ J/m for $Ni_{80}Fe_{20}$); r_{max} and r_{min} are the outer and inner radii of the vortex core, respectively. Here, r_{max} can be approximated as the ring width and r_{min} is equal to the magnetic exchange length ($\delta \sim 4$ nm). Taking $M_S \sim 8.0 \times 10^5$ A/m, the estimated sum of the two differences for S660, S500, and S340 samples is -11.56, -8.40, and -5.29×10^{-17} J, respectively. The negative sign for all the samples indicates that, in comparison to TDW, the VDW has lower energy in them. Thus, the nucleation of VDW is favorable than the growth of TDW at point A in the M(H). Further reduction of the field will lead to the growth of both the VDWs to the size of ring width. Decreasing the field further exerts pressure on both the diagonally opposite VDWs and depins the one that is relatively weak pinned. This entire process of nucleation, growth, and depinning of VDW represents overcoming an effective energy barrier in the first step (A to B) of OS to VS transition.[15] In the second step (B to C), decreasing the field slightly below B pushes the depinned VDW rapidly towards the other VDW, at point C both annihilate each other giving rise to a zero stray field VS. The increase of H_{C1} and H_{C2} with decrease in either temperature or ring width may thus reflect an increase of effective energy barrier for VDW depinning. This is well supported by the observed enhancement of the first step of OS to VS transition with decrease of both temperature and ring width (compare various A to B regions in Figs. 1(b), 1(d), and 1(f)).

Figs. 3(c) and 3(d) depict M_r/M_s versus T plots for all three samples. The sample S660 practically shows $M_r/M_s \sim 0$ at all the temperatures (see Fig. 3(c)). The sample S500 shows similar trend for $300 < T < 150$ K (see Fig. 3(c)). However, at $T < 150$ K, M_r/M_s increases rapidly up to 0.68 at 3 K. As also mentioned above, this reflects a evolution of remanent state from VS to OS with decrease in temperature (see M(H) in Fig. 1(d)). The sample S340 shows high values of M_r/M_s at all T between 3 and 300 K (Fig. 3(d)) reflecting OS as the remanent state in the entire temperature range. We may conclude that the magnitude of M_r/M_s is a good indicator of the nature of remanent state in ring structures.

In Fig. 4(a) we plot M(H) loops with field applied at different out-of-plane angles for sample S340 at 300 K. Interestingly, with increasing θ (Fig. 4(a)) the M(H) loops shrink along the M-axis and expand along the H-axis. At $\theta = 90°$, the M(H) loop is virtually hysteresis free and lies nearly flat on the H-axis. These results suggest strong in-plane anisotropy of magnetization in mesoscopic ring lattices as seen in permalloy films. To check this hypothesis, we plot in Fig. 4(b) the in-plane component $H\cos\theta$ vs. in-plane magnetization $M/\cos\theta$. The rescaled results show considerable overlap of the M(H) data at various angles indicating that the in-plane anisotropy is indeed retained after mesoscopic patterning. Note also that the position of point B is nearly unchanged in the rescaled M(H) curves. Few deviations, for instance, change in net positive moment in the VS and values of M_s with angle in the rescaled plots are also evident. Both H_{C1} and H_{C2} increase monotonically with angle (see insets of Fig. 4(b)). The rescaled values $H_{C1}\cos\theta$ and $H_{C2}\cos\theta$, plotted in the same insets, do tend to become angle independent, however, with a shallow dip at $\theta \sim 40°$ within the margin of the error. The most likely reason for deviation from perfect scaling could be the interaction of out-of-plane

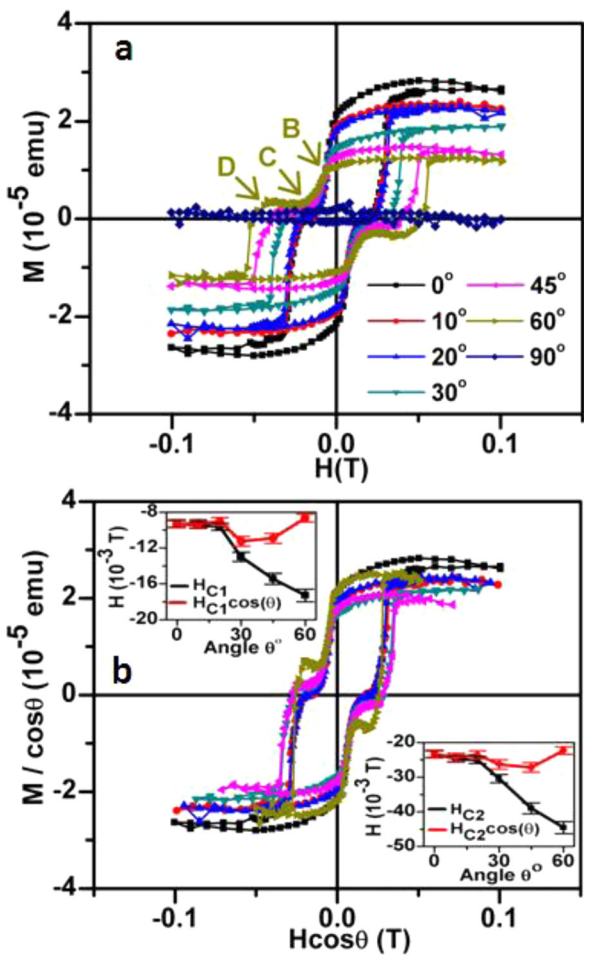

FIG. 4. M(H) at 300 K at various fixed angles $\theta = 0$ to 90° for S340 sample: (a) as measured and (b) rescaled $M/\cos\theta$ versus $H\cos\theta$. The points B, C, and D are indicated for M(H) at $\theta = 60°$. Insets of (b) show angle dependence of H_{C1} and $H_{C1}\cos\theta$ and H_{C2} and $H_{C2}\cos\theta$.

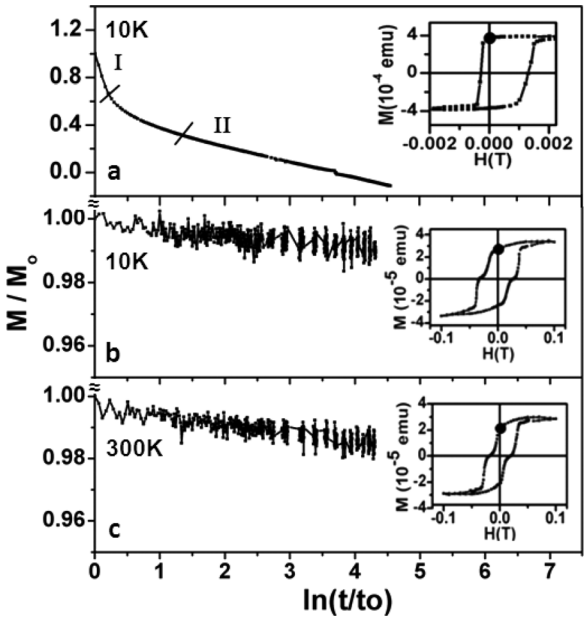

FIG. 5. Decay of M/M_o as a function of $\ln(t/t_o)$ for: (a) plain film at 10 K; and S340 sample at (b) 10 K and (c) 300 K. The corresponding M(H) loops are shown in the insets. The dot on the M(H) loop marks the starting magnetic state after switching the field off (at $t = t_o$).

magnetized core of the VDW with out-of-plane field component at different angles. Very few studies of angular dependence in the magnetic rings have been reported that too only for in-plane field rotation.[20,21] A decrease of H_{C1} with angle and a symmetrical minimum at 45° was reported for ring arrays.[20] Large and no variation in the values of H_{C1} and H_{C2} as a function of angle, respectively, was reported for single ring.[21]

The relaxation of remanent magnetization as a function of time for plain film at 10 K, and S340 sample at 10 and 300 K are plotted in Figs. 5(a), 5(b) and 5(c) respectively. The starting magnetic state after switching the field off (at $t = t_o$) is marked by a dot in the corresponding M(H) curves (see insets of Fig. 5). The magnetization is expected to relax as:[22]

$$M(t) = M(t_0)\left[1 - \frac{k_B T}{U_0}\ln(t/t_0)\right], \qquad (3)$$

where M(t) and $M(t_0)$ are the magnetization at the time t and t_o, and U_0 is the energy barrier. For plain thin film at 10 K (see Fig. 5(a)), the remanent magnetized state gets completely relaxed and demagnetized in the experimental time scale. The data can be fitted by Eq. (3) in two separate time windows marked as "I" and "II" with estimated $U_0/T \sim 0.052$ and 0.66 meV/K, respectively. Whereas in the sample S340, over similar experimental time window, the remanent magnetized state relaxes logarithmically to less than 1% of its starting value (see Figs. 5(b) and 5(c)). The estimated values of U_0/T at 10 and 300 K are ~50 and 32 meV/K, respectively, which are over two orders of magnitude higher than that of plain film, signifying the temporal stability of the remnant OS in mesoscopic ring structures.

IV. CONCLUSIONS

In conclusion, arrays of non-interacting permalloy submicron rings were fabricated and their magnetization was studied as a function of ring width, temperature, angle, and time. All the samples showed a double step transition from OS to VS, indicating the VDW formation and dynamics in the OS. The increase of critical reversal fields H_{C1} and H_{C2} with decrease in ring width and temperature seems to be related with the energy barrier for VDW depinning. The angular scaling of the M(H) reveals that the in-plane field component is mainly responsible for the magnetic properties. Magnetic relaxation measurements demonstrate that the remanent OS is highly robust even at a bath temperature of 300 K.

ACKNOWLEDGMENTS

This research has been supported by the Council of Scientific and Industrial Research and Department of Science and technology (DST), Government of India. R.C.B. acknowledges J. C. Bose National Fellowship of the DST.

[1]S. D. Bader, Rev. Mod. Phys. **78**, 1 (2006).
[2]R. P. Cowburn, D. K. Koltsov, A. O. Adeyeye, M. E. Welland, and D. M. Tricker, Phys. Rev. Lett. **83**, 1042 (1999).
[3]J. K. Ha, R. Hertel, and J. Kirschner, Phys. Rev. B **67**, 224432 (2003).
[4]M. Natali, A. Lebib, Y. Chenb, I. L. Prejbeanu, and K. Ounadjela, J. Appl. Phys. **91**, 7041 (2002).
[5]J. Rothman, M. Kläui, L. L. Diaz, C. A. F. Vaz, A. Bleloch, J. A. C. Bland, Z. Cui, and R. Speaks, Phys. Rev. Lett. **86**, 1098 (2001).
[6]M. Kläui, C. A. F. Vaz, L. Lopez-Diaz, and J. A. C. Bland, J. Phys.: Condens. Matter **15**, R985 (2003).
[7]C. A. F. Vaz, T. J. Hayward, J. Llandro, F. Schackert, D. Morecroft, J. A. C. Bland, M. Kläui, M. Laufenberg, D. Backes, U. Rudiger, F. J. Castano, C. A. Ross, L. J. Heyderman, F. Nolting, A. Locatelli, G. Faini, S. Cherifi, and W. Wernsdorfer, J. Phys.: Condens. Matter **19**, 255207 (2007).
[8]A. V. Goncharov, A. A. Zhukov, V. V. Metlushko, G. Bordignon, H. Fangohr, G. Karapetrov, B. Llic, and P. A. J. de Groot, J. Appl. Phys. **99**, 08Q508 (2006).
[9]A. Subramani, D. Geerpuram, A. Domanowski, V. Baskaran, and V. Metlushko, Physica C **404**, 241 (2004).
[10]Z. G. Guo, L. Q. Pan, H. M. Qiu, M. Y. Rafique, and S. Zeng, Adv. Mater. Res. **710**, 80 (2013).
[11]J. Sautner, N. Jahedi, and V. Metlushko, *Electromagnetic, Magnetostatic, and Exchange-Interaction Vortices in Confined Magnetic Structures*, edited by E. O. Kamenetskii (Transworld Research Network, Trivandrum, 2008), p. 427.
[12]T. Miyawaki, K. Toyoda, M. Kohda, A. Fujita, and J. Nitta, Appl. Phys. Lett. **89**, 122508 (2006).
[13]M. Kläui, J. Phys.: Condens. Matter **20**, 313001 (2008).
[14]J. Wang, A. O. Adeyeye, and N. Singh, Appl. Phys. Lett. **87**, 262508 (2005).
[15]T. A. Moore, T. J. Hayward, D. H. Y. Tse, J. A. C. Bland, F. J. Castano, and C. A. Ross, J. Appl. Phys. **97**, 063910 (2005).
[16]M. Kläui, L. L. Diaz, J. Rothman, C. A. F. Vaz, J. A. C. Bland, and Z. Cui, J. Magn. Magn. Mater. **240**, 7 (2002).
[17]F. J. Castano, C. A. Ross, A. Eilez, W. Jung, and C. Frandsen, Phys. Rev. B **69**, 144421 (2004).
[18]R. D. McMichael and M. J. Donahue, IEEE Trans. Magn. **33**, 4167 (1997).
[19]W. Zhang and S. Haas, Phys. Rev. B **81**, 064433 (2010).
[20]E. Tadmor, Y. J. Rosen, I. K. Schuller, and S. Bar-Ad, J. Appl. Phys. **112**, 103903 (2012).
[21]M. Kläui, C. A. F. Vaz, J. A. C. Bland, E. H. C. P. Sinnecker, A. P. Guimaraes, W. Wernsdorfer, G. Faini, E. Cambril, L. J. Heyderman, and C. David, Appl. Phys. Lett. **84**, 951 (2004).
[22]J. Tejada, J. M. Hernández, E. del Barco, and X. X. Zhang, Contributions to Science **1**(1), 25 (1999).